DEEP INELASTIC ν SCATTERING

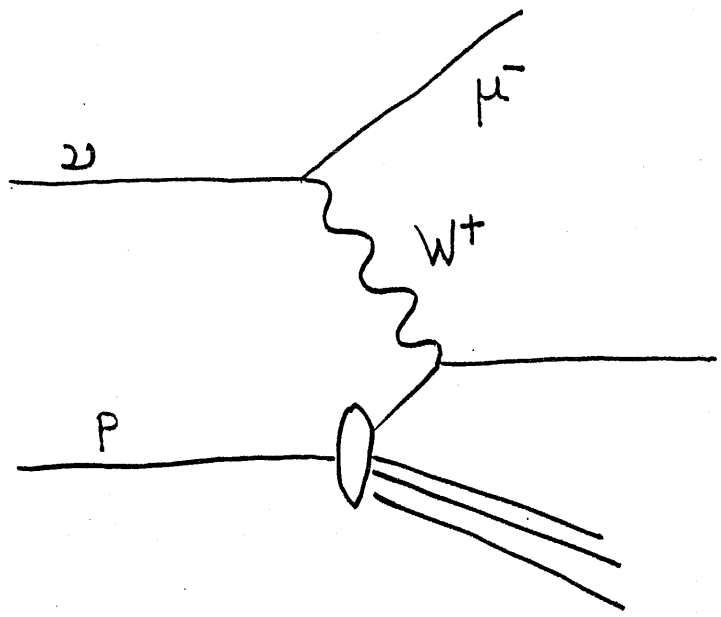

Charged Current ν Scattering.

The procedure for obtaining an expression for ν scattering is similar to that for charged lepton scattering: we take pointlil neutrino scattering, expressing the amplitude for the process as a produc of two tensors. The charged fermior momentum distribution is then related tc the $q_i(x)$.

NEUTRINO-ELECTRON SCATTERING

The full matrix element for $\nu_\mu e^- \to \mu^- \nu_e$, taking into account the W^+ propagator, is

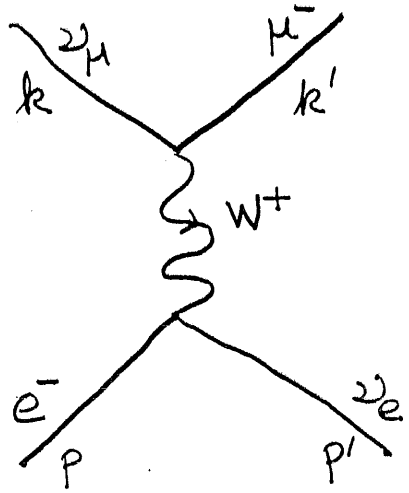

$$A = \frac{g^2}{2}\bar{u}(\mu)\gamma_\mu\frac{(1-\gamma_5)}{2}u(\nu_\mu)\left[\frac{-g^{\mu\nu}+q^\mu q^\nu/M_W^2}{q^2-M_W^2}\right]\bar{u}(\nu_e)\gamma_\nu\frac{(1-\gamma_5)}{2}u(e)$$

Typical fixed target Q^2 values for fixed target ν scattering make the second propagator term negligible. We obtain the FERMI form

$$\frac{G_F}{\sqrt{2}}\bar{u}(\mu)\gamma_\mu(1-\gamma_5)u(\nu_\mu)\,g^{\mu\nu}\,\bar{u}(\nu_e)(1-\gamma_5)u(e)$$

with

$$\frac{G_F}{\sqrt{2}} = g^2\frac{1}{8M_W^2}$$

After some effort, $|A|^2$ can be written as a product of traces

$$|A|^2 = \mathrm{Tr}\left[\not{k}'\gamma_\mu(1-\gamma_5)\not{k}\gamma_\nu(1-\gamma_5)\right]\frac{1}{2}\mathrm{Tr}\left[\not{p}'\gamma^\mu(1-\gamma_5)\not{p}\gamma^\nu(1-\gamma_5)\right]$$

This is of the form

$$|A|^2 = \left(\frac{G_F^2}{2}\right) N_{\mu\nu}\, E^{\mu\nu}$$

$N_{\mu\nu}$, $E^{\mu\nu}$ refers to the upper (ν) and lower (e) vertices respectively.

Note that TRACE CALCULATIONS normally come about through spin averaging. For NEUTRINOS, there is no spin averaging, as all neutrinos are LEFT-HANDED (spin and momentum *anti*parallel)

However, the trace method provides a useful way of performi the calculation, and the factor $(1-\gamma_5)$ acts as a projection operator, selec left-handed states only.

In this way we have

$$N_{\mu\nu} = \mathrm{Tr}[\not{k}'\gamma_\mu(1-\gamma_5)\not{k}\gamma_\nu(1-\gamma_5)]$$

and

$$E^{\mu\nu} = \frac{1}{2}\mathrm{Tr}[\not{p}'\gamma^\mu(1-\gamma_5)\not{p}\gamma^\nu(1-\gamma_5)]$$

$E^{\mu\nu}$ has spin averaging (factor $\frac{1}{2}$), but $N_{\mu\nu}$ does not.

22 STRUCTURE FUNCTIONS (Cont.)

The quantity $|A|^2$ for the process $\nu_\mu e^- \to \mu^- \nu_e$ is found to factorize into a product of two tensors:-

$$|A|^2 = \left(\frac{G_F^2}{2}\right) N_{\mu\nu} E^{\mu\nu}$$

The tensors $N_{\mu\nu}$ and $E^{\mu\nu}$ refer to the neutrino and electron vertices respectively. They can be evaluated using trace techniques, because the projection operators $(1-\gamma_5)$ ensure only the required helicity states are non-zero.

(2)

Evaluating the NEUTRINO tensor

$$N_{\mu\nu} = 8\left[k'_\mu k_\nu + k'_\nu k_\mu + (q^2/2) g_{\mu\nu} - i \epsilon_{\mu\nu\alpha\beta} k^\alpha k'^\beta\right]$$

Here $\epsilon_{\alpha\beta\gamma\delta}$ is the *totally antisymmetri rank 4 tensor*

$$\epsilon_{\alpha\beta\gamma\delta} = \begin{cases} +1 & \text{for } \epsilon_{0123} \text{ and even permutations of } 0,1,2,3 \\ -1 & \text{for } \epsilon_{1023} \text{ and odd permutations of } 0,1,2,3 \\ 0 & \text{otherwise} \end{cases}$$

This is still too complicated.

Current conservation [ATTCHISON & HEY §3.8.2] leads to the condition

$$q^\mu N_{\mu\nu} = q^\nu N_{\mu\nu} = 0$$

which may be invoked to simplify the ELECTRON tensor $E^{\mu\nu}$ (which we shall

(3)

shortly modify for quarks.

This reads

$$E^{\mu\nu} = 4\left[p'^{\mu}p^{\nu} + p'^{\nu}p^{\mu} + (q^2/2)g^{\mu\nu} - i\epsilon^{\mu\nu\gamma\delta}p_\gamma p'_\delta\right]$$

We may now write

$$p' = p + q$$

and drop all terms involving q, as they will vanish in the contraction of the tensors. [The exception is the antisymmetric term, where $\epsilon^{\mu\nu\gamma\delta}p_\gamma p_\delta$ vanishes

Thus we obtain

$$E^{\mu\nu}_{eff} = 8p^{\mu}p^{\nu} + 2q^2 g^{\mu\nu} - 4i\epsilon^{\mu\nu\gamma\delta}p_\gamma q_\delta$$

This now gives us the functional form for ν structure functions

$$W^{\mu\nu}_{(\nu)} = -g^{\mu\nu}W_1^{(\nu)} + \frac{1}{M^2}p^{\mu}p^{\nu}W_2^{(\nu)} + \frac{i}{2M^2}\epsilon^{\mu\nu\gamma\delta}p_\gamma q_\delta W_3^{(\nu)}$$

Compare this form

$$W^{\mu\nu}_{(\nu)} = -g^{\mu\nu} W_1^{(\nu)} + \frac{1}{M^2} p^\mu p^\nu W_2^{(\nu)} + \frac{i}{2M^2} \epsilon^{\mu\nu\gamma\delta} p_\gamma q_\delta W_3^{(\nu)}$$

with the corresponding hadronic tensor for electromagnetic interactions

$$W^{\mu\nu}_{(\ell)} = (-g^{\mu\nu} + q^\mu q^\nu / q^2) W_1^{(\ell)}$$

$$+ \frac{1}{M^2}\left[p^\mu - [(p\cdot q)/q^2] q^\mu\right]\left[p^\nu - [(p\cdot q)/q^2] q^\nu\right] W_2^{(\ell)}$$

We see that the terms are similar. The terms in red in $W^{\mu\nu}_{(\ell)}$ arise from the propagator. Similar structures would appear in $W^{\mu\nu}_{(\nu)}$ if we had not simplified the expression to the Fermi form.

The antisymmetric term with $W_3^{(\nu)}$ in $W^{\mu\nu}_{(\nu)}$ is a NEW structure function arising from the parity-violating nature of the weak interaction

Our aim in studying ν interactions was to find independent relations for the quark distribution functions. To simplify this, for the time being we ignore strangeness changing currents, i.e. we set the Cabibbo angle to zero.

Thus the W^+ couples to the d and the $\bar{u}$, while the W^- couples to the u and the $\bar{d}$.

ν BEAM

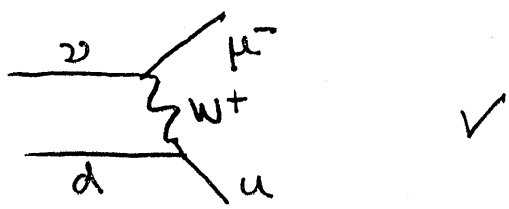

✓

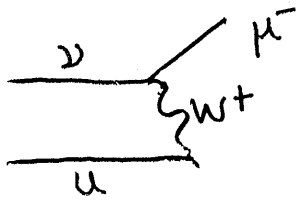

X

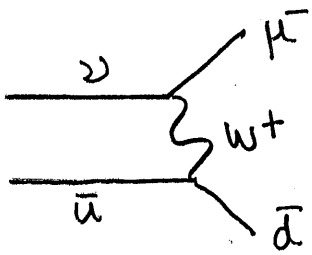

✓

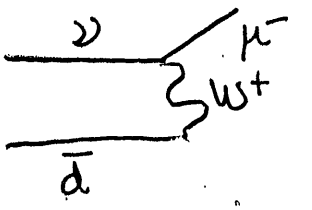

X

$\bar{\nu}$ BEAM

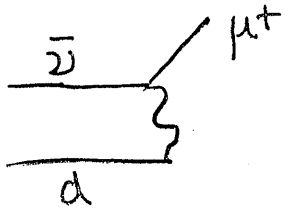

X

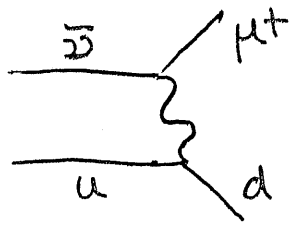

✓

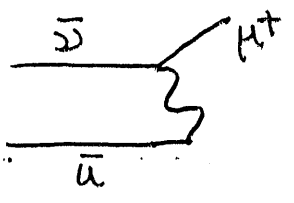

X

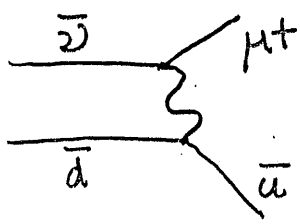

✓

(6)

The Bjorken y distributions provide a way to study the quark distributions. Even at the (anti) neutrino – (anti) quark level they fall into two distinct groups:-

$$\frac{d\sigma}{dy}\left[\nu\bar{q}\,;\,\bar{\nu}q\right] \sim (1-y)^2$$

$$\frac{d\sigma}{dy}\left[\nu q;\,\bar{\nu}\bar{q}\right] \sim 1 \qquad \text{(Isotropic)}$$

We now write the ν ($\bar{\nu}$) cross section in terms of Bjorken variables, using the Callan-Gross relation to put F_1 in terms of F_2

$$\frac{d^2\sigma^{\bar{\nu}}_{\nu}}{dxdy} = \frac{G^2 s}{2\pi} F_2^{(\nu)}(x)\left[\frac{(1+(1-y)^2)}{2} \mp \frac{(1-(1-y^2))}{2}\frac{x F_3^{(\nu)}(x)}{F_2^{(\nu)}(x)}\right]$$

[CLOSE eq. [11.41]]

This suggests the following parton model interpretation:-

$$\frac{d^2\sigma_{\nu}}{dxdy} = \frac{2G^2 M E_\nu x}{\pi}\left[\sum_i g_i^2 f_i(x) + \sum_j g_j^2 \bar{f}_j(x)(1-y)^2\right]$$

[RENTON eq. [7.104]]

Comparing terms

$$F_2(x) = 2\sum_{ij}\left[g_i^2 x q_i(x) + g_j^2 x \bar{q}_j(x)\right]$$

$$xF_3(x) = 2\sum_{ij}\left[g_i^2 x q_i(x) - g_j^2 x \bar{q}_j(x)\right]$$

$g_i = \cos\theta_c$
$g_j = \sin\theta_c$

Writing this out in detail,

$$F_2^{\nu p} = 2x\left[\bar{u}(x) + d(x) + s(x) + \bar{c}(x)\right]$$

$$F_2^{\bar{\nu} p} = 2x\left[u(x) + \bar{d}(x) + \bar{s}(x) + c(x)\right]$$

$$xF_3^{\nu p} = 2x\left[d(x) + s(x) - \bar{u}(x) - \bar{c}(x)\right]$$

$$xF_3^{\bar{\nu} p} = 2x\left[u(x) - \bar{d}(x) - \bar{s}(x) + c(x)\right]$$

Another possibility is to consider scattering from an ISOSCALAR target, i.e. one with the same number of proton and neutron targets.

In this case we obtain

$$2xF_1^{\nu N}(x) = F_2^{\nu N}(x) = 2xF_1^{\bar{\nu} N}(x) = F_2^{\bar{\nu} N}(x) \equiv \tfrac{1}{2}\left[F_2^{\nu p}(x) + F_2^{\nu n}\right.$$

$$= \sum_i x\left[f_i(x) + \bar{f}_i(x)\right]$$

$$xF_3^{\nu N}(x) = xF_3^{\bar{\nu} N}(x) = \tfrac{1}{2}\left[xF_3^{\nu p}(x) + xF_3^{\nu n}(x)\right]$$

$$= \sum_i x\left[f_i(x) - \bar{f}_i(x)\right]$$

For comparison, the corresponding expressions for *charged* lepton scattering are

$$2xF_1^{lp}(x) = F_2^{lp}(x) = e_u^2 x\left[u(x)+\bar{u}(x)\right] + e_d^2\left[d(x)+\bar{d}(x)\right]$$

$$+ e_s^2\left[s(x)+\bar{s}(x)\right] + e_c^2\left[c(x)+\bar{c}(x)\right.$$

[PROTON TARGET]

$$F_2^{lN}(x) \equiv \tfrac{1}{2}\left(F_2^{lp}(x)+F_2^{ln}(x)\right) = \tfrac{1}{2}\left(e_u^2+e_d^2\right)x\left[u(x)+\bar{u}(x)+d(x)+\bar{d}\right.$$

$$+ e_s(x)\left[s(x)+\bar{s}(x)\right] + e_c^2\left[c(x)+\bar{c}(x)\right.$$

[ISOSCALAR TARGET]

(9) Note that if the dominant process is scattering off u and d quarks (for both ν and ℓ scattering), then the F_2 structure functions are related by

$$\frac{F_2^{\ell N}(x)}{F_2^{\nu N}(x)} \simeq \frac{1}{2}\left(e_u^2 + e_d^2\right) = \frac{5}{18}$$

This relation has been tested extensively. The small offset increases above charm threshold, as expected.

Notice that, since $f_i^{(sea)}(x) = \bar{f}_i^{(sea)}(x)$ when the u and d quark distributions dominate, the expansion of $xF_3^{(\nu N)}(x)$ becomes

$$xF_3^{\nu N}(x) = x\left[u(x) + d(x) - \bar{u}(x) - \bar{d}(x)\right] = x\left[u_v(x) + d_v(x)\right]$$

i.e. $xF_3^{\nu N}(x)$ picks out the valence quark contribution.

The preceding list of relations allows one to extract the quark momentum distributions.

However the process is long and laborioas as the number of equations is still small. One starts BECOW charm threshold, and fits for the u and d quark distributions. Then the Q^2 is increased and a second iteration started, this time includin charm. The Q^2 behaviour of the distribation functions (Q^2 EVOLUTION) is well understood in terms of the ALTARELLI-PARISI equations.

SUM RULES REVISITED

The work just done allows us to put forward some more complicated sum rules. Note that the QPM derivations are not rigorous. Some of the sum rules are also derivable from current algebra, in which case they are exact.

1. GROSS LLEWELLYN-SMITH SUM RULE

Measures number of valence quarks in the nucleon

$$\int_0^1 \frac{1}{x} \cdot x F_3^{\nu N}(x)\, dx = \int_0^1 (u_V(x) + d_V(x))\, dx$$

$$= 3$$

[N.B. There are perturbative QCD corrections:

$$\int_0^1 \frac{1}{x} \cdot x F_3^{\nu N}(x)\, dx = 3\left(1 - \frac{\alpha_s}{\pi}\right)$$

where $\alpha_s(Q^2)$ is the strong coupling constant.]

2. GOTTFRIED SUM RULE

This is sensitive to the quark charges. Assuming only u and d quarks contribute (simple form)

$$\int \frac{1}{x}\left[F_2^{lp}(x) - F_2^{ln}(x)\right] dx = (e_u^2 - e_d^2)\left[u + \bar{u} - d - \bar{d}\right]$$

$$= \frac{1}{3}\left[u_v + u_s + \bar{u} - d_v - d_s - \bar{d}\right]$$

$$= \int \frac{1}{3}\left[u_v - d_v\right] dx = \frac{1}{3}$$

3. MOMENTUM SUM RULE

$F_2^{\nu N}(x)$ is represented by

$$F_2^{\nu N}(x) = x(u + \bar{u} + d + \bar{d} + s + \bar{s} + \dots)$$

Note that the expectation value for a variat x is given by

$$\langle x \rangle = \int x\, P(x)\, dx$$

where $P(x)$ is the probability density function for x.

2. GOTTFRIED SUM RULE

This is sensitive to the quark charges. Assuming only u and d quarks contribute (simple form)

$$\int \frac{1}{x}\left[F_2^{ep}(x) - F_2^{en}(x)\right] dx = (e_u^2 - e_d^2)\left[u + \bar{u} - d - \bar{d}\right]$$

$$= \frac{1}{3}\left[u_v + u_s + \bar{u} - d_v - d_s - \bar{d}\right]$$

$$= \int \frac{1}{3}\left[u_v - d_v\right] dx = \frac{1}{3}$$

3. MOMENTUM SUM RULE

$F_2^{\nu N}(x)$ is represented by

$$F_2^{\nu N}(x) = x(u + \bar{u} + d + \bar{d} + s + \bar{s} + \dots)$$

Note that the expectation value for a varial x is given by

$$\langle x \rangle = \int x\, P(x)\, dx$$

where $P(x)$ is the probability density function for x.

This means

$$\int_0^1 F_2^{\nu N}(x)\,dx = \sum_i \langle x_{q_i} \rangle$$

is the total momentum fraction carried by quarks and antiquarks.

If a nucleon consists of only quarks (and antiquarks)

$$\int_0^1 F_2^{\nu N}(x)\,dx = 1$$

However, experimentally,

$$\int_0^1 F_2^{\nu N}(x)\,dx \simeq 0.5$$

This means 50% of the nucleon momentum is carried by constituents (i) which do not feel the weak interaction, nor (ii) the electromagnetic interaction (since $F_2^{lp} = 5/18\, F_2^{\nu p}$ works well).

Historically, this was important evidence for the existence of GLUONS.

QCD CORRECTIONS

1. The "naive Quark Parton Model" (QPM) assumes deep inelastic scattering is describable in terms of quarks, photons and IVBs.

2. The model works quite well at the Q^2 values used in the SLAC experiments of the 1970's.

3. As Q^2 increases, QCD corrections become more important. The scales involved can be seen through the DE BROGLIE wavelength

$$\lambda \simeq \hbar/Q$$

Using $\hbar = 197$ MeV fermi, we see that for $Q^2 = 1\ \text{GeV}^2$ $\lambda \sim 1/5$ fermi, or 1/5 the "radius" of a proton.

For Q^2 in this range, partonic structure begins

For $Q^2 \gg 1\,\text{GeV}^2$, further structure is revealed, through gluon radiation and quark loops.

4. The fact that the "further structure" consists of further quarks and gluons reflects the current belief that these are the smallest level of structure

5. To see this, compare what happens one level up. Hadrons were once believed to be the most fundamental objects. For $Q^2 \gtrsim 1\,\text{GeV}^2$, hadrons show themselves to have structure, NOT consisting of hadrons.

If, for some Q^2, we reveal substructure in quarks and gluons, above this value a description in terms of more gluon emission would be inadequate.

6. Corrections are also required to take into account the effects of bound states (e.g. diquark scattering, target mass effects and other "higher twist" effects. As mentioned earlier, these have a $1/Q^2$ dependence, i.e. their effect becomes LESS important as Q^2 increases. Intuitively, we may think of the structure as "fragile", and therefore more likely to break as Q^2 gets larger.

7. To gain some insight into how the non-higher-twist terms will behave with Q^2. We depict the lowest level hadron vertex as

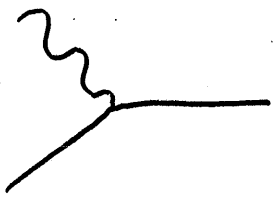

④ This may be modified through gluon emission

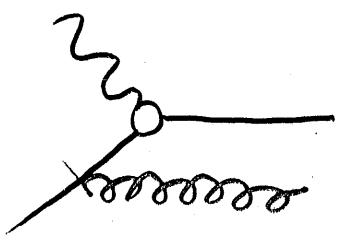

or pair production

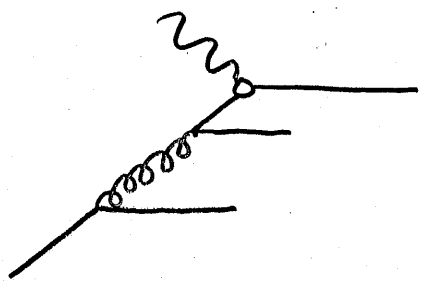

... and so forth. Intuitively, extra partons are produced through these QCD processes, and thus the momentum fraction carried by any given hadron is REDUCED. Therefore, we expect structure functions to SOFTEN as Q^2 increases, i.e. move to smaller x values.

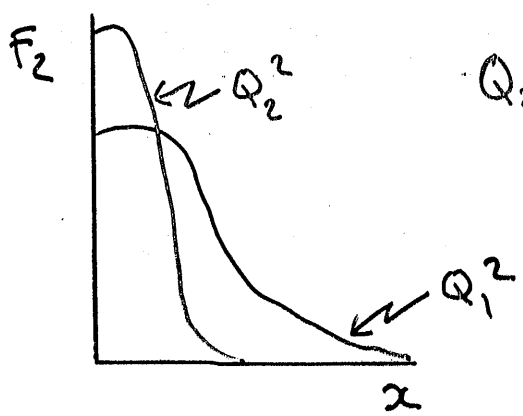

Thus, if $F_2(x_0)$ is plotted against Q^2 for different values of x_0, we see

(i) at LOW x, $F_2(x)$ INCREASES with increasing Q^2.

(ii) at HIGH x, $F_2(x)$ DECREASES with increasing Q^2

However, note that these effects are SMALL corrections to the phenomenon of BJORKEN SCALING, i.e. the slopes $\partial \ln F_2(x) / \partial \ln Q^2$ are small.

Note that in principle as we go to higher Q^2 we enter a region where *perturbative* QCD is valid. This means that Feynman diagram techniques analogous to those used in QED can be used.

However the validity of QCD perturbative calculations is ALWAYS more dubious than their QED counterparts.

This is because the strong interaction coupling constant α_s is in fact quite large (~ 0.2)

In fact α_s ITSELF decreases as Q^2 increases.

GLUON RADIATION

Gluon radiation corrections are an important class of corrections to basic QPM corrections.

One of the simplest diagrams of this type is

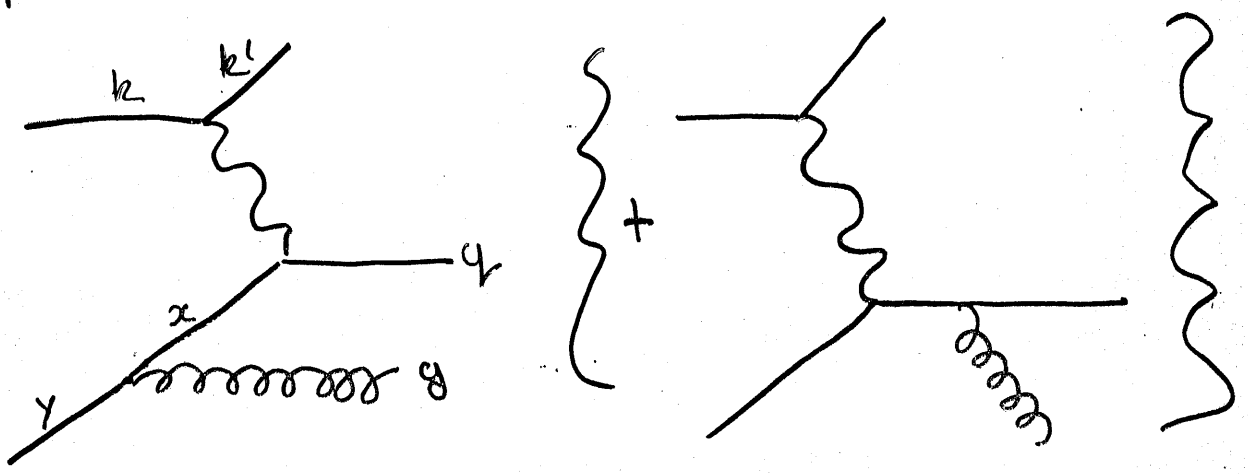

Here initially the incoming parton carries a fraction y of the proton's momentum. After emission of a gluon, a softer quark with momentum fraction x ($x<y$) goes on to interact with the incoming virtual photon.

If this were the whole story, one could apply the Feynman rules, then note the correction

Unfortunately, the comparatively large value of α_s means that the NEXT ORDER of corrections, e.g.

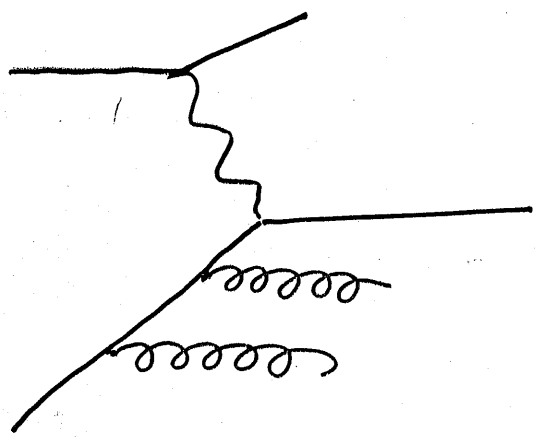

are not necessarily much smaller. (But the EVALUATION of the diagrams is considerably longer and more difficult.)

(9) Many QCD corrections have only been calculated to leading order.

This may be because

(i) it is not possible to do any better

(ii) it is hoped that the functional dependence of the corrections is correctly represented, and

(iii) it is hoped that the next-to-leading order terms, when available, will not alter the physical picture.

However, in many cases where next-to-leading order terms become available, it has turned out that (ii) and (iii) are NOT satisfied. (and therefore may STILL not be satisfied.)

ALTARELLI - PARISI EQUATIONS

In the case of the quark distribution functions themselves, it is possible to treat the problem recursively, so as to obtain a solution to all levels

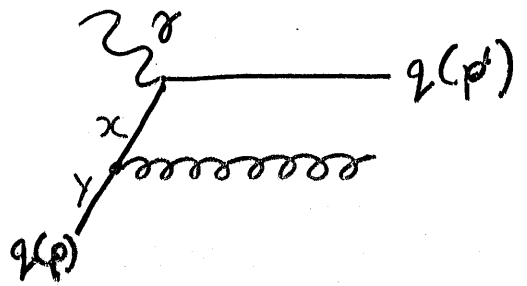

In the example shown earlier, we may describe the quark with momentum fraction x as being "inside" the one with momentum fraction y. The probability for this is governed by the momentum splitting function $P_{qq}(x/y)$, which is calculable in QCD.

Integrating over all momentum sharings Altarelli and Parisi obtained a differential equation

$$\frac{dq(x,Q^2)}{d\ln Q^2} = \frac{\alpha_s}{\pi}\int_x^1 \frac{dy}{y}\, q(y,Q^2)\, P_{qq}(x/y)$$

However, things are more complicated, as the first quark may itself be "inside" a gluon carrying a higher momentum fraction

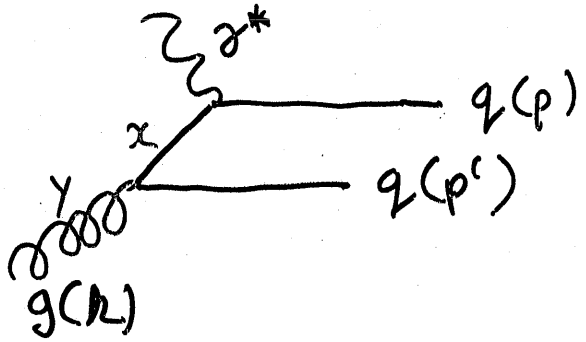

Here the momentum sharing is governed by a different momentum splitting function $P_{qg}(x/y)$. So the Full differential equation becomes

$$\frac{d\, q_i(x,Q^2)}{d \ln Q^2} = \frac{\alpha_s(Q^2)}{2\pi} \int_x^1 \frac{dy}{y} \left[P_{qq}(x/y) q_i(y,Q^2) + P_{qg}(x/y) g(y,Q^2) \right]$$

Here $q_i(x,Q^2)$, $g(x,Q^2)$ are the quark and gluon distribution functions at a given Q^2.

The equation gives the "EVOLUTION" of the quark distribution function $q_i(x,Q^2)$ with Q^2.

However, as we have invoked a GLUON probability function $g(x, Q^2)$, we need a corresponding evolution equation. This is,

$$\frac{dg(x,Q^2)}{d\ln Q^2} = \frac{\alpha_s(Q^2)}{2\pi}\int_x^1 \frac{dy}{y}\left[\sum_j P_{gq_j}(x/y)\,q_j(y,Q^2)\right] + P_{gg}(x/y)\,g(y,Q^2)$$

where we take into account the "running" coupling constant, $\alpha_s(Q^2)$

$$\alpha_s(Q^2) = \frac{12\pi}{(33-2n_f)\ln(Q^2/\Lambda^2)} + O\left(\ln\ln(Q^2/\Lambda^2)\right)$$

The Altarelli-Parisi equations form a set of coupled differential equations which may be solved numerically. They need a set of values of the $q_j(x, Q^2)$ at some Q^2 as starting values, but then allow calculation at any other Q^2, provided Q^2 is not too low.

Once the solutions have settled, one also gets the gluon distribution function $g(x, Q^2)$

(13) The beauty of this method is that it covers these processes to all orders, i.e. complicated diagrams such as

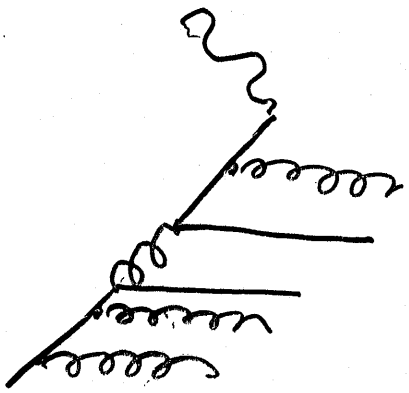

are automatically taken into account.

However, corrections of the Higher Twist type are NOT taken into account.

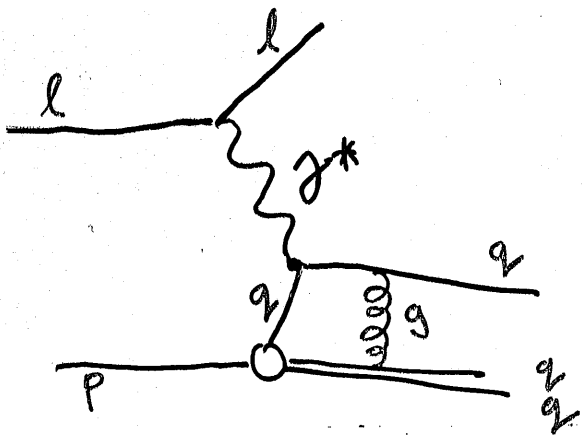

(1)

STRUCTURE FUNCTIONS BY OTHER MEANS

THE DRELL-YAN PROCESS

The chief limitation of deep inelastic scattering as a probe of hadron structure is that only STABLE hadrons, which can be used as targets, can be studied, (Except COHERENT PRODUCTION) i.e. only PROTONS and NEUTRONS.

Using these measurements, organized into quark distribution functio as input, the study of the DRELL-YAN PROCESS provides a way to measure the quark distribution functions for other hadrons.

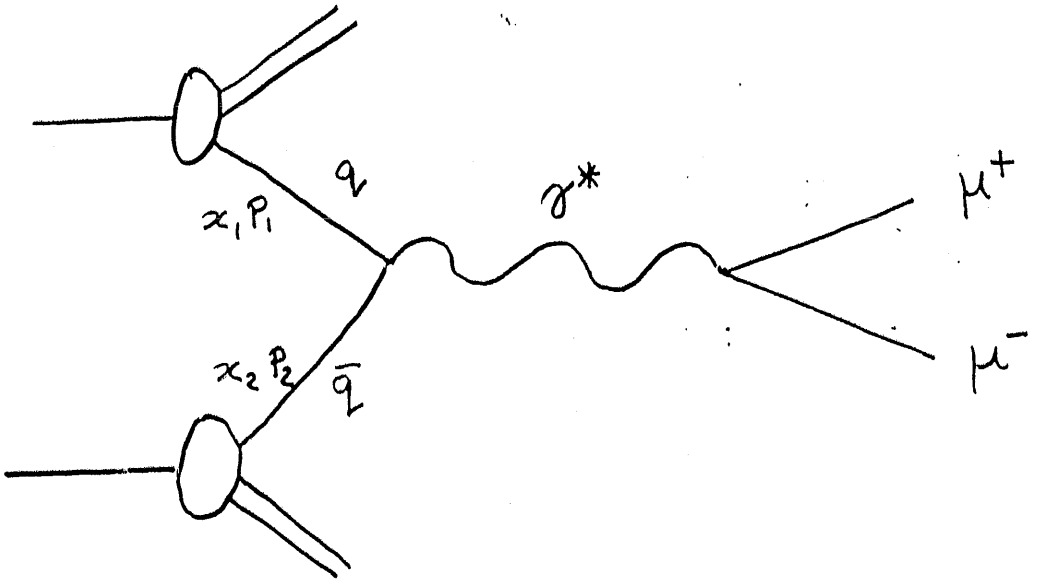

DRELL-YAN KINEMATICS

Work at LOW p_T. q and $\bar{q}$ carry momentum fractions x_1, x_2 of their respective hadron's momenta. The virtual photon has 4 vector

$$(E, p) = ((x_1+x_2)P, 0, 0, (x_1-x_2)P)$$

(in overall CM, where $\underline{P}_1^* = -\underline{P}_2^* = P$)

So

$$q^2 = 4 x_1 x_2 P^2 = x_1 x_2 s$$

and $x_F(\gamma^*) = 2q_z/s^{1/2} = x_1 - x_2$

Standard techniques exist for organizing this expression into a product of two traces

$$\frac{1}{4}\sum_{s,r}\sum_{s'r'}|F_{sr;s'r'}|^2 = \left(\frac{e^2}{q^2}\right)^2 \left\{\frac{1}{2}\mathrm{Tr}[(\not{k}'+m)\gamma_\mu(\not{k}+m)\gamma_\nu]\right\} \times \left\{\frac{1}{2}\mathrm{Tr}[(\not{p}'+m)\gamma^\mu(\not{p}+m)\gamma^\nu]\right\}$$

$$\equiv \left(\frac{e^2}{q^2}\right)^2 L_{\mu\nu}\, M^{\mu\nu}$$

Note that the traces correspond to two tensors, one for the electron and one for the muon.

$$L_{\mu\nu} = 2\left[k'_\mu k_\nu + k'_\nu k_\mu + (q^2/2) g_{\mu\nu}\right]$$

$$M^{\mu\nu} = 2\left[p'^\mu p^\nu + p'^\nu p^\mu + (q^2/2) g^{\mu\nu}\right]$$

(performing the traces). Finally the products of 4 vectors are calculated.

(11) In the LAB frame the result of this (laborious) contraction is

$$L_{\mu\nu} M^{\mu\nu} = 16 M^2 E E' \left\{ \cos^2 \frac{\theta}{2} - \frac{q^2}{2M^2} \sin^2 \frac{\theta}{2} \right\}$$

We now move to the introduction of structure functions in 3 logical steps.

- Scattering from a STRUCTURELESS proton.

  Same form as above. (Still scattering of structureless fermions.)

- Elastic electron proton scattering.

  The matrix element has the same form as before. However the proton tensor is replaced by

$$L^{\mu\nu}_{(p)} = \frac{1}{2} \mathrm{Tr} (\not{p}' + m) \Gamma^\mu (\not{p} + m) \Gamma^\nu$$

NOTE This kinematics is very similar to that for DOUBLE POMERON scattering

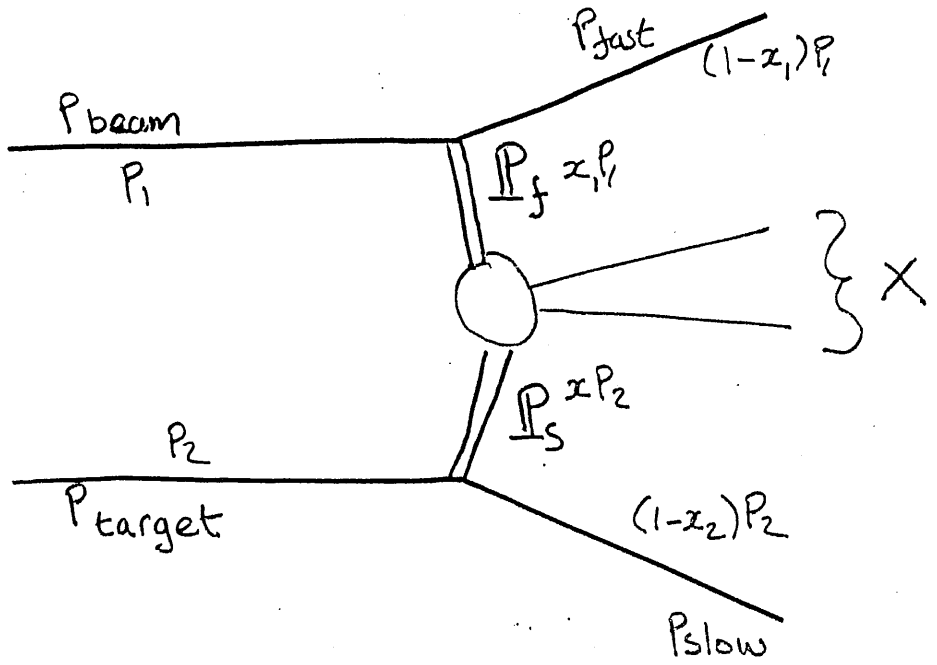

$$M^2 \left(\rightleftharpoons q^2_{DY}\right) = 4x_1x_2P^2 = x_1x_2s$$

The FEYNMAN x of the "fast" and "slow" particles is the fraction of the maximum longitudinal momentum they carry (in the CM). This is, for (e.g.) the "fast" particle

$$\frac{P^*_{fast}}{P^*} = \frac{(1-x_1)P_1}{P_1} = (1-x_1) = x_F(fast)$$

Thus as $x_F(fast) \to 1$, $x_F(slow) \to -1$, the effective mass M decreases

Returning to DRELL-YAN, the cross section for the parton level process $q_1 \bar{q}_2 \to \mu^+ \mu^-$ is well understood

$$\frac{d\hat{\sigma}}{dq^2}(q_1 \bar{q}_2 \to \mu^+ \mu^-) = \frac{4\pi\alpha^2}{3} \cdot e_i^2 \cdot \frac{1}{q^2} \cdot \delta(q^2 - x_1 x_2 s)$$

The cross section for the HADRONIC process is the convolution of the parton level process over all possible sharings of the parton momenta :-

$$\frac{d\sigma}{dq^2}(h_1 h_2 \to X \ell_1 \ell_2)$$

$$= \frac{1}{3} \sum_i \int dx_1 dx_2 \left[q_i(x_1) \bar{q}_i(x_2) + \bar{q}_i(x_1) q_i(x_2) \right] \frac{d\hat{\sigma}}{dq^2}$$

$$= \frac{1}{3} \sum_i \int dx_1 dx_2 \left[q_i(x_1) \bar{q}_i(x_2) + \bar{q}_i(x_1) q_i(x_2) \right] \frac{4\pi\alpha^2}{3q^2} e_i^2 \delta(q^2 - x_1 x_2 s)$$

This expression can be re-arranged using the Dirac δ-function property

$$\delta(f(x)) = \frac{\delta(x-x_0)}{\left|\, df/dx \,\right|_{x=x_0}} \quad : f(x_0)=0$$

to put the argument of the δ-function as a difference of two *dimensionless* terms.

How? Write $\delta(q^2 - x_1 x_2 s)$ in terms of the DIMENSIONLESS variable $\omega = s/q^2$

$$q^2 - x_1 x_2 s = f(\omega) = (s/\omega - x_1 x_2 q^2 \omega)$$

Then $$\frac{df}{d\omega} = -\frac{s}{\omega^2} - x_1 x_2 q^2$$

$f(\omega)=0$ when $\omega = \frac{1}{x_1 x_2}$ or $\omega^2 = \frac{s}{q^2 x_1 x_2}$

so $$\left.\frac{df}{d\omega}\right|_{\omega_0} = \left(-\frac{s q^2}{s} x_1 x_2 - x_1 x_2 q^2\right) = -2 x_1 x_2 q^2$$

so $$\delta(f(\omega)) = \frac{\delta\left(\frac{1}{x_1 x_2} - \omega\right)}{-2 x_1 x_2 q^2}$$

(6)

$$\frac{d\sigma}{dq^2} = \frac{1}{6}\sum_i \int dx_1 dx_2 \left\{ \frac{q_i(x_1)}{x_1}\frac{\bar{q}_i(x_2)}{x_2} + \frac{\bar{q}_i(x_1)}{x_1}\frac{q_i(x_2)}{x_2} \right\} \frac{4\pi\alpha^2 e_i^2}{3q^4} \times \delta\left(\frac{1}{x_1 x_2} - \frac{s}{q^2}\right)$$

This can be rewritten in the dimensionless form

$$q^4 \frac{d\sigma}{dq^2}\left(\equiv M^4 \frac{d\sigma}{dM^2}\right) = \sum_i \int dx_1 dx_2 \left\{ q_i(x_1)\bar{q}_i(x_2) + \bar{q}_i(x_1) q_i(x_2) \right\} \frac{4\pi\alpha^2 e_i^2}{3} \delta\left(\frac{1}{\tau} - \frac{1}{x_1 x_2}\right)$$

$$= g(\tau)$$

$$\tau = 1/\omega = M^2/s$$

Note:

1. Drell-Yan cross sections should SCALE in the variable τ, in a way similar to Bjorken scaling in Deep Inelastic Scattering.
2. Drell-Yan cross section formula provides access to many new quark distribution functions.
3. The formula allows the ABSOLUTE cross section for Drell Yan production to be calculated.

- Prediction (1) seems to work quite well.

- Observation (2) also works quite well. The general form can be tested by studying ratios such as

$$R = \frac{\sigma(\pi^+ A \to \mu^+\mu^- X)}{\sigma(\pi^- A \to \mu^+\mu^- X)}$$

where A is an ISOSCALAR target (e.g. ^{12}C).

For small x, production from sea quarks is favoured, so π^+ and π^- are equivalent and $R \sim 1$

For large x, production from VALENCE quarks dominates. Here the $\pi^+(u\bar{d})$ picks out d quarks in the target, and the $\pi^-(\bar{u}d)$ picks out u quarks. As the target has equal numbers of each, $R \sim \left(\frac{e_d}{e_u}\right)^2 = 1/4$

(8) The quark distribution functions for (e.g.) the $\pi^{\pm}$ can be determined by giving them a parametric form, e.g.

$$q_{\alpha\beta}(x) = x^{\alpha}(1-x)^{\beta} \quad ,$$

performing the integrals in the cross section formula, and fitting data for α and β. The nucleon distributions are introduced from Deep Inelastic Scattering, but can be checked for consistency through Drell Yan continuum production in pp scattering.

All this works quite well.

Observation (3) does NOT work very well in practice.

It is customary to parameterize the disagreement in terms of K-factors. These are given by

$$K = \frac{\sigma_{DY:\,exp.}}{\sigma_{DY:\,theo.,\,leading\,order}} \sim 2.3$$

In fact the theoretical predictions can be made much better. The improvement comes in the partonic sub-process, where in addition to the basic process $q\bar{q}$ such QCD corrections

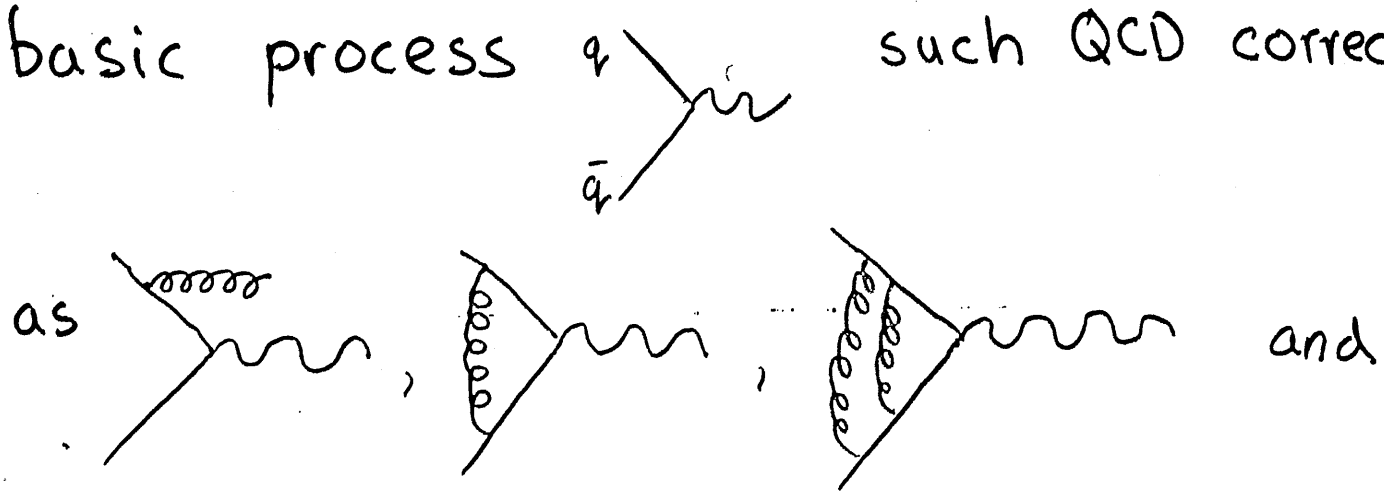

as , , and so on are considered.

These corrections give a predicted K factor of around 2, (which is not bad), but have a similar behaviour as functions of the quark distribution parameters to the leading order term.

Note that we have assumed $p_T \sim 0$. If $p_T \neq 0$ (e.g. because of the primordial k_T of partons in the nucleon) other processes giving rise to a virtual γ may contribute.

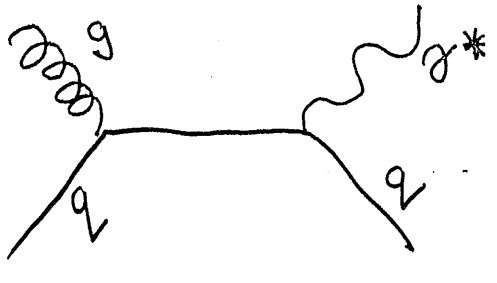

QCD Compton

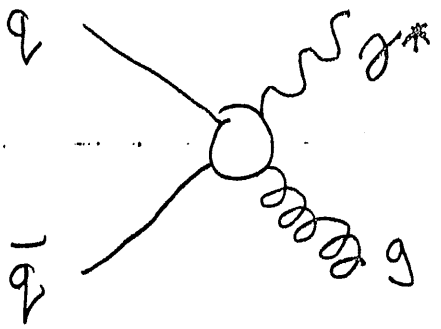

Annihilation

ANGULAR DEPENDENCE

Returning to the leading order [QPM] term, it is also possible to determine the angular dependence of the μ^+ in the $\mu^+\mu^-$ rest frame.

The starting point is once again the fermion-fermion scattering process

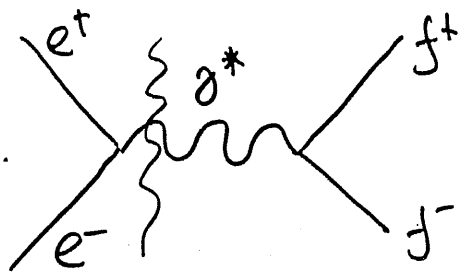

where the e^+e^- annihilation serves as a source of virtual photons. Once again one obtains a product of tensors $L_{\mu\nu}L^{\mu\nu}$, but this time the 4-vectors are evaluated in the $\mu^+\mu^-$ rest frame, not the LAB frame.

The result is

$$\frac{d\sigma}{d\Omega} = \frac{e_i^2 \alpha^2 \beta}{4s} (2 - \beta + \beta \cos^2\theta)$$

As $\beta \to 1$ (relativistic limit)

$$\frac{d\sigma}{d\Omega} \sim (1 + \cos^2\theta)$$

This is in effect a measure of the POLARIZATION of the virtual photon. The "logarithmic" (gluon radiation) QCD terms do not alter the prediction, which is very well satisfied in practice. Deviations CAN be found with high statistics data owing to HIGHER TWIST effects.

Fig. 14.9. Scaling shown by saihe data as in Fig. 14.8 when plotted against m^2/s. (From Vannucci, 1978.)

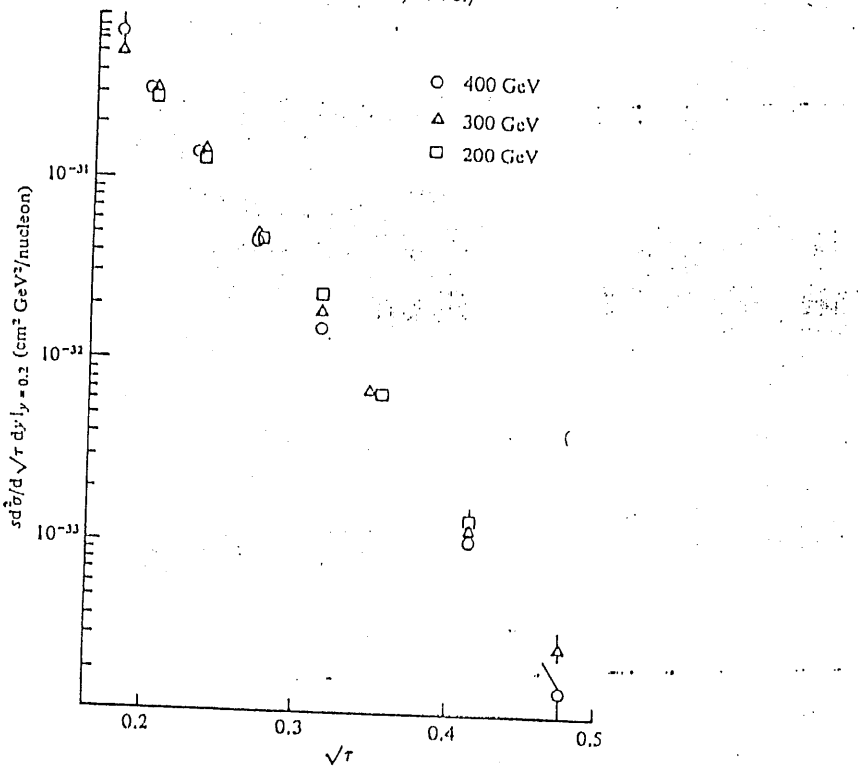

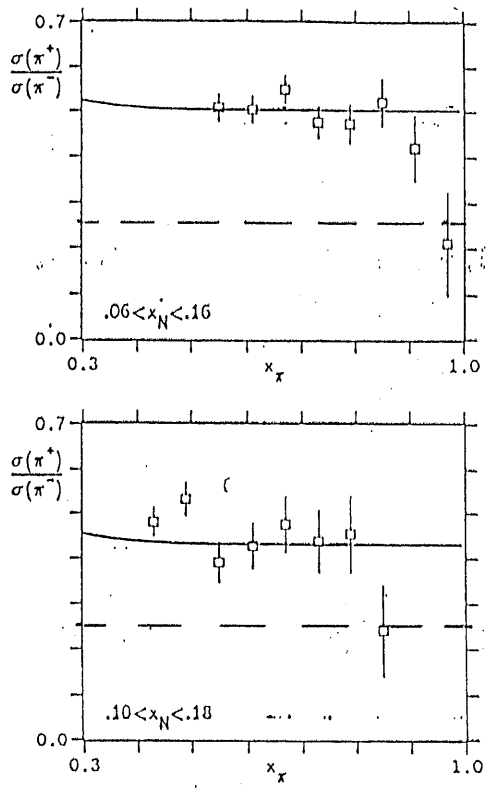

FIG. 2. The ratio of cross sections for muon-pair production by π^+ and π^- beams at 253 GeV as a function of x_π. The restrictions on x_N derive from cuts on the pair mass to avoid muons from resonance decay. The smooth curves are Drell-Yan model predictions using the pion structure function from analysis of our π^- data [8] and nucleon structure functions from Duke Owens [12] (second set).

Duke and Owens.[12] Recall that in the Drell-Yan model the ratio $\sigma(\pi^+)/\sigma(\pi^-)$ would be 1/4 if we could ignore sea quarks, and if $Z = A/2$.

On the whole, the agreement with the Drell-Yan model is excellent, with the exception of the point at $x_\pi = 0.96$ which is about 2.5 standard deviations below the model.

If we accept fig. 2 as evidence that the Drell-Yan model applies to that data, we can extract the proton sea-quark distribution, S_p. As we wish to avoid the use of proton valence-quark distributions measured in other experiments, we report only the ratio

$$\frac{S_p(x_N)}{V_p^u(x_N) + V_p^d(x_N)}.$$

Our determination of this ratio is plotted as a function of x_N in fig. 3. For comparision the experimental results of the CDHS collaboration[13] are also shown; they studied deep-inelastic scattering with ν_μ and $\bar{\nu}_\mu$ beams. Our data provide an improved measure of the sea-quark distribution in the region $x_N < 0.1$.

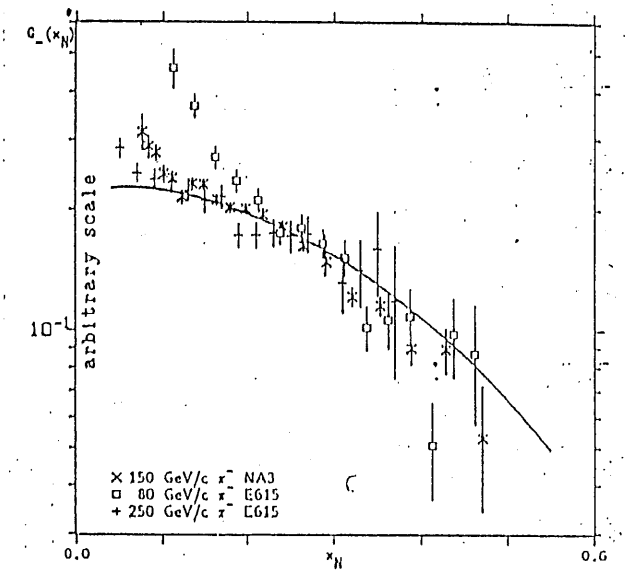

FIG. 4. The nucleon structure function $G^-_N(x_N)$ as measured in $\pi^- N \to \mu^+\mu^- X$ at 80 [7] 150 [15] and 253 [8] GeV. The curve is from the Duke-Owens nucleon structure functions [12]. The three sets of measured points have been normalized to the curve at $x_N = 0.25$.

To subtract the effect of the vector mesons, the cross sections were binned on a grid of x_π-x_N. The bin size in x_π was 0.02, and the bin size for x_N was 0.01 for $x_N < 0.16$ and 0.02 for $x_N > 0.16$. According to (A3), for a slice at fixed x_π, x_N is proportional to M^2, which permits a resonance subtraction to be made at each slice of x_π. For this the x_N bins were subdivded into smaller intervals whose width corresponded to about 50 MeV/c^2 in mass. The subtraction was greatest at low x_π, and was almost negiligble near $x_\pi = 1$ (the region which corresponds to low x_N at a given mass). Figure 5 gives an impression of the quality of the subtraction procedure at the extremes of the region of x_π used in the analysis.

The subtracted cross sections were then used to determine the pion and nucleon structure functions, using the procedure described in ref. 8. An x_π-x_N bin was used only if it was entirely within the specified mass limits. The latter were $M < 8.55$ GeV/c^2 and $M > 3.2$, 3.6, or 4.0 GeV/c^2. There are about 36,000 pairs with mass above 4.0 GeV/c^2, and 70,000 with mass above 3.2 GeV/c^2.

The pion valence structure function, $V_\pi(x_\pi)$, was determined in a fit to the grid of cross sections $d\sigma/dx_\pi dx_N$ assuming the nucleon quark distributions have the form found by the CCFRR collaboration,[16] and assuming QCD evolution of these distributions as parametrized by Buras and Gaemers.[17] Following the Berger-Brodsky model[4] the pion structure function was parametrized as

$$V_\pi(x_\pi) = x_\pi^\alpha (1 - x_\pi)^\beta + \gamma \frac{2x_\pi^2}{9M^2_{\mu\mu}}.$$

An overall normalization factor, K, was left as a parameter so the the pion and nucleon structure functions could be normalized to 1 when interpreted as probability distributions. (This requires an assumption as to the fraction of the pion's momentum carried by gluons,